Electrodeposition of Cu on PEDOT for a Hybrid Solid-State Electronic Device

Martina Vizza [1,2], **Giulio Pappaianni** [1], **Walter Giurlani** [1,2], **Andrea Stefani** [3], **Roberto Giovanardi** [3], **Massimo Innocenti** [1,2,4,5] and **Claudio Fontanesi** [3,*]

1   Department of Chemistry "Ugo Schiff", University of Florence, Via della Lastruccia 3, 50019 Sesto Fiorentino, Italy; martina.vizza@unifi.it (M.V.); giulio.pappaianni@stud.unifi.it (G.P.); walter.giurlani@unifi.it (W.G.); minnocenti@unifi.it (M.I.)

2   National Interuniversity Consortium of Materials Science and Technology (INSTM), Via G. Giusti 9, 50121 Firenze, Italy

3   Department of Engineering 'Enzo Ferrari', University of Modena and Reggio Emilia, Via Vivarelli 10, 41125 Modena, Italy; andrea.stefani@unimore.it (A.S.); roberto.giovanardi@unimore.it (R.G.)

4   Insititute of Chemistry of Organometallic Compounds (ICCOM)—National Research Council (CNR), Via Madonna del Piano 10, 50019 Sesto Fiorentino, Italy

5   Center for Colloid and Surface Science (CSGI), Via della Lastruccia 3, 50019 Sesto Fiorentino, Italy

*   Correspondence: claudio.fontanesi@unimore.it

Abstract: Conductive polymers are nowadays attracting great attention for their peculiar mechanical, electrical and optical proprieties. In particular, PEDOT can be used in a wide range of innovative applications, from electroluminescent devices to photovoltaics. In this work, the electrochemical deposition of 3,4 ethylenedioxythiophene (EDOT) was performed on various substrates (ITO, thin films of gold and palladium on silicon wafers) by means of both potentiostatic and potentiodynamic techniques. This was intended to further expand the applications of electrochemically deposited PEDOT, particularly regarding the preparation of thin films in tight contact with electrode surfaces. This allows one to obtain systems prone to be used as electrodes in stacked devices. Chronoamperometric experiments were performed to study the nucleation and growth process of PEDOT. SEM, ESEM and AFM analysis allowed the characterization of the morphology of the polymeric films obtained. Raman and visible spectroscopy confirmed the high-quality of the coatings on the different substrates. Then, the PEDOT films were used as the base material for the further electrodeposition of a copper layer. In this way, a hybrid electronic device was obtained, by using electrochemical methods only. The high conductivity and ohmic behavior of the device were confirmed over a wide range of frequencies with electrical impedance spectroscopy analysis.

Keywords: PEDOT; electrosynthesis; hybrid solid-state electronic device; Cu electrodeposition; Raman; visible spectroscopy; SEM; AFM; polymer coating

1. Introduction

Conductive polymers (CPs) constitute an important class of materials, which combine some mechanical characteristics of plastics with the typical electrical properties of semiconductors; these polymeric species contain conjugated bonds, which give rise to almost continuous valence and conduction bands. Furthermore, many CPs are characterized by optical transparency in the oxidized state and by a modulable band gap [1]. This means that these polymers can be useful in multiple applications, including catalysis [2], electroluminescent devices [3–5], organic transistors [6–11], LEDs [12–15] and photovoltaic polymer cells [16–23]. CPs also exhibit good adhesion to electrode surfaces [24]. For these reasons, the field of conductive polymers has attracted the interest of many scientists since their discovery [2]. Compared to inorganic semiconductors, CPs offer further advantages, such as a low switching time [25], a high contrast ratio (CR) [26] and a modulable bandgap [24]. The chemical, electrochemical oxidation or reduction of the polymeric chains

of CPs generate charge centers, which are responsible for the electrical conductivity of these species [27]. A significant research area related to CPs concerns the preparation of optically transparent polymers, easily subjected to both n-type and p-type doping and highly conductive in the doped state.

Among the numerous conductive polymers, polyanilines, polypyrroles, polythiophenes, polyphenylenes and poly (p-phenylene vinylenes) are of particular importance. In particular, the polyaniline family is characterized by low cost and the possibility of being obtained in the bulk form. However, the possible presence of benzidines in the polymer backbone, which can lead to the formation of toxic (carcinogenic) products by degradation, considerably limits the applications of polyaniline and derivatives. Heteroaromatic polypyrroles, polythiophenes and poly (p-phenylenes vinylenes) are more environmentally friendly systems, still presenting the disadvantages of being insoluble and non-fusible. To overcome these problems, an attempt was made to obtain derivatives of these polymeric species. By modifying the structure of the main polymer chain and the chemistry of the side groups, alternative CPs with a great variety of properties have been developed [28].

One of the most important conductive polymers is poly (3,4 ethylenedioxythiophene) (PEDOT), which can be obtained by synthetic or electrochemical processes. By means of electropolymerization, it is possible to obtain polymeric films of high morphological quality, with small quantities of the initial monomer and short polymerization times. PEDOT can be synthetized by chemical or electrochemical polymerization of 3,4-ethylenedioxythiophene (EDOT), a thiophene derivative with positions 3 and 4 blocked by an ethylenedioxy group [28,29]. The most important reactions of EDOT are those of oxidation, typically with the result of producing conductive oligomers and polymeric materials in the presence of doping counterions (anions), which balance the charges [8]. Among the organic conductive polymers, polythiophenes and their derivatives, such as PEDOT, are of particular interest due to their high stability. In particular, PEDOT presents multiple advantages over unsubstituted polythiophenes. Indeed, the introduction of the ethylenedioxy substituents in positions 3 and 4 of the monomeric ring of EDOT prevents α,β and β,β couplings during the polymerization process. Consequently, the resulting polymer is more defined from a regiochemical point of view. Furthermore, the electrochemical synthesis of PEDOT is facilitated compared to that of an unsubstituted polythiophene. This occurs since the oxidative potential of EDOT is lower than that of thiophene [1,28]. Therefore, PEDOT has established itself as one of the most important materials among conductive polymers and has acquired great popularity in the scientific community. Many research groups have focused on PEDOT chemistry in recent years, bringing about an exponential increase in the number of patents and publications. This material features a unique combination of properties: high conductivity ($\approx$300 S/cm) [19,30], good transparency in thin films [3,7] and low bandgap (1.6–1.7 eV) [31]. These characteristics make PEDOT films suitable for optoelectronic and hybrid electronics applications, allowing the preparation of organic/inorganic interfaces without the need of high-cost vacuum techniques [32].

In this work, the electrochemical polymerization of PEDOT was investigated to further expand the range of possible uses of PEDOT. In that, electrochemically grown polymers, with respect to chemically synthesized ones, allow for the preparation of thin films in tight contact with electrode surfaces. In this way, systems prone to be used as electrodes in stacked devices can be obtained. Moreover, electrochemically grown polymers were quite recently exploited in obtaining intrinsically grown chiral PANI, thus paving the way for the preparation of 2D layered materials to be used in spintronic devices. [33,34]. Potentiostatic and potentiodynamic electrochemical depositions were performed on various substrates: indium tin oxide (ITO) glass and silicon wafers coated with thin films of gold and palladium. The obtained PEDOT coatings were characterized by environmental scanning electron microscopy (ESEM), scanning electron microscopy (SEM), atomic force microscopy (AFM) and visible and Raman spectroscopy. Then, the polymeric films were further used as working electrodes, undergoing a copper metallization. In this way, a hybrid electronic device was obtained, by using electrochemical methods only. The conductivity and the

ohmic behavior of the samples were characterized by means of electrochemical impedance spectroscopy (EIS).

2. Materials and Methods

Sigma Aldrich 3,4-ethylenedioxythiophene 97% (EDOT), Sigma Aldrich copper (II) sulfate $CuSO_4 \geq 99\%$, Sigma Aldrich sulfuric acid $H_2SO_4 \geq 99.9\%$, Thermo Fisher ACS reagent grade $LiClO_4 \geq 95\%$ and Sigma Aldrich ACS reagent grade acetonitrile (ACN) $\geq 99.5\%$ were used without further purification. The EDOT polymerization studies and the copper metallization were performed in a one-compartment, three-electrode electrochemical cell. Three different substrates were used as working electrodes: ITO (1×2 cm^2), gold and palladium supported on silicon (1.5×1.5 cm^2). The counter-electrode was a Pt wire, and an Ag wire was used as pseudo-reference. The solutions were de-aerated by bubbling N_2 for 15 min before each electrochemical experiment, which was performed under N_2 atmosphere at room temperature. Prior to each electropolymerization process, the working electrodes were cleaned by sonication in EtOH, then rinsed with AcOH and distilled water and finally dried with N_2. The electropolymerization studies, deposition of PEDOT and metallization with copper were performed by means of cyclic voltammetry and chronoamperometry in unstirred solutions. The electropolymerization solution consisted of 10 mM EDOT and 0.1 M $LiClO_4$ in ACN. The copper metallization was carried out in an aqueous solution of 1.5 M H_2SO_4 and 0.5 M $CuSO_4$ (measured pH oscillating between 1 and 1.5). The electrochemical experiments were performed by means of a Metrohm μAUTOLABIII (Herisau, Switzerland). EIS measurements were recorded in air using a 2-electrode configuration, in the region of frequency 10^4–0.1 Hz. Samples were contacted to the electrodes using silver paste. Sinusoidal amplitude (Vrms) of 0.01 V, from 100 kHz to 0.1 Hz, with 10 samplings per decade, were used. No additional DC bias was applied between the electrodes. The microscopic characterization of PEDOT films was carried out using an environmental scanning electron microscope (ESEM; Quanta-200, Fei Company, Oxford Instruments (High Wycombe, UK). The scanning electron microscopy analysis and the focused ion beam (FIB) ablation were performed by means of a GAIA 3 instrument equipped with Triglav electron and gallium FIB Cobra Gallium columns manufactured by Tescan (Brno, Czech Republic). Atomic force microscopy measurements were carried out in contact mode with a Si_3N_4 triangular cantilever (Veeco, NP-S10, Munich, Germany) on a PicoSPM (Molecular Imaging, AZ, USA). The spectrophotometric measurements on the PEDOT films on ITO were performed by means of UV–VIS Cary 300 Agilent Technology (Santa Clara, CA, USA). Raman spectra were obtained by a Jobin Yvon LabRAM confocal Raman microscope (Horiba, Darmstadt, Germany) with a Peltier cooled CCD detector. A solid state 532 nm, with 60 mW maximum power, was used.

2.1. Potentiodynamic Growth

In the potentiodynamic deposition, the film was grown by repeatedly cycling potentials between −0.6 V and 1.3 V, with a sweep rate of 50 mV/s. Figure 1a shows 8 consecutive CVs scans of EDOT solution on the gold electrode. In the first CV scan, the oxidative onset potential was at 1.1 V, and then the current density increased, reaching a maximum value at 1.3 V. Starting from the second CV scan, the onset oxidative process shifted at lower potentials and set at 1.0 V in the last cyclic voltammetry. This suggests that the repeated deposition of PEDOT promotes monomer oxidation, facilitating the formation of the polymer coating on the gold electrode. The current density peak increased with every cycle.
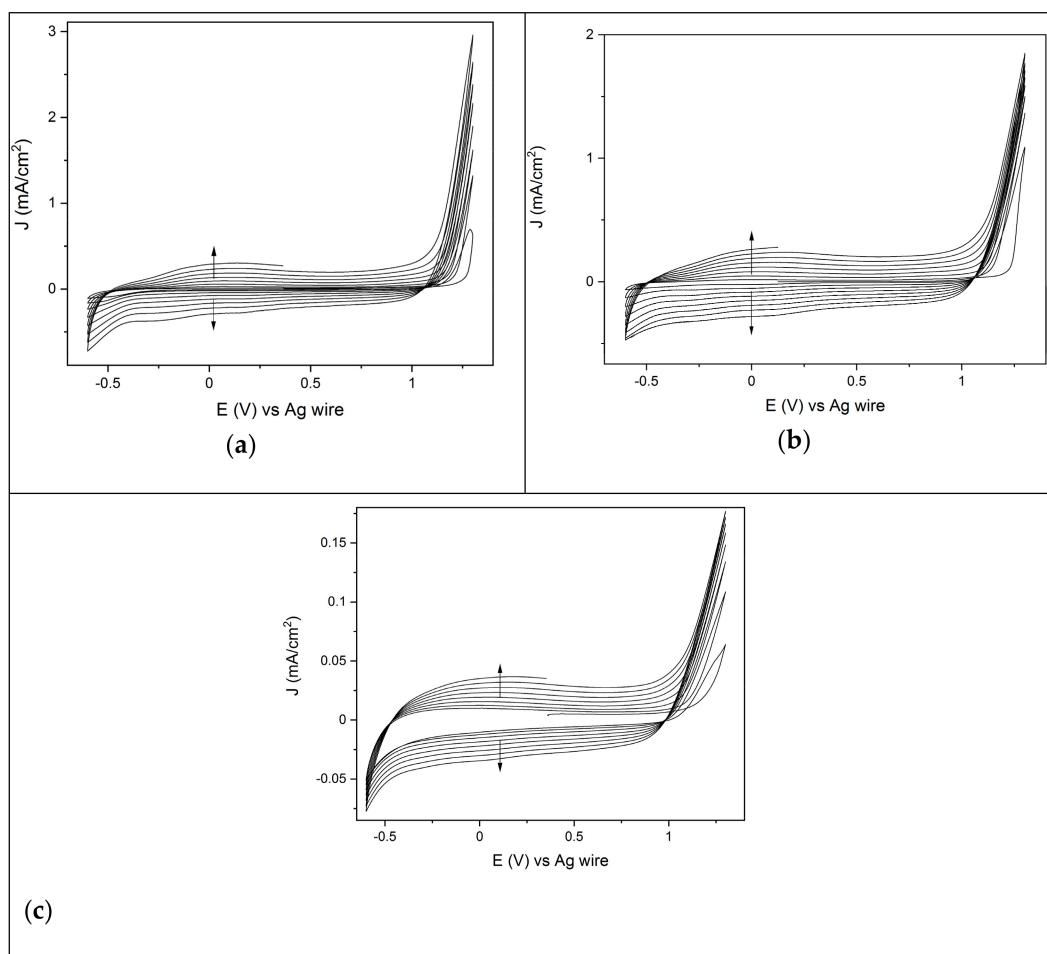
Figure 1. Eight consecutive CVs of the EDOT solution between −0.6 V and 1.3 V, starting from the OCP, scan rate 50 mV/s, on the various substrates: (**a**) gold, (**b**) palladium and (**c**) ITO.

Indicating the continuous growth of the PEDOT film on the substrate. Furthermore, deposition after deposition, the current density range of the CVs widened, with an increase of both cathodic and anodic current. This capacitive effect arose from the continuous growth of the electroactive polymeric film on the electrode, with a thickness that increased scan after scan [35].

The trend of PEDOT deposition on the palladium electrode (Figure 1b) was like that previously described. However, the maximum current density value in the first CV scan was significantly higher than the one registered on gold (Figure 1a). This may suggest that the formation of the polymer coating is favored on the Pd electrode, with a higher amount of the PEDOT film deposited after the first CV scan. A homogeneous blue polymer coating was obtained after 8 CVs scans on both gold and palladium. The electropolymerization of PEDOT on ITO differed significantly from the one that took place on the metal electrodes. The onset oxidation potential was still at 1.1 V, but the overall current density values were definitely lower (Figure 1c). Furthermore, the first 4 CVs showed a crossover of the reverse cathodic scan over the anodic one, bringing about the so called "nucleation loop". In particular, the current density of the reverse scan was higher than the anodic one in the region between the switching potential and the onset oxidative potential (1.1–1.3 V). This phenomenon has been interpreted as being due to polymer nucleation effects [36] or, more recently, to homogeneous reactions involving the starting monomer and the oligomer follow-up product [37]. The nucleation loop disappeared from the fifth CV on (Figure 1c), being replaced by the growth of the polymeric nuclei previously deposited. At the end of the potentiodynamic polymerization, non-homogeneous dark blue spots of PEDOT covered the surface of the immersed area of the electrode. Therefore, the potentiody-

namic route does not seem to be the optimum process to obtain PEDOT films on ITO. However, the potentiodynamic route set the basis for further investigation of PEDOT deposition by means of potentiostatic methods. Indeed, the detection of the onset oxidation potential and the maximum current density values in Figure 1 allowed us to look for the optimum conditions to obtain the PEDOT film potentiostatically on the different electrodes. Of note was the presence of two isoamperic point potentials found during the scans on all the different substrates (Figure 1), the one at cathodic potentials (−0.5 V) and the other at anodic ones (1 V) [38].

2.2. Potentiostatic Growth

The potentiostatic deposition of PEDOT on Au, Pd and ITO was studied by means of chronoamperometric experiments. Before each potentiostatic polymerization, the working electrode was switched from the open circuit potential (OCP) to 0.8 V for 5 s. This step allows for the formation of a double-layer charge between the electrode and the solution interface [39]. Under these experimental conditions, the adsorption of the monomer is absent or negligible [40]. Then, the EDOT polymerization was performed by polarizing the electrode for 30 s at different potentials, in the range between 1.1 V and 1.3 V (Figure 2).
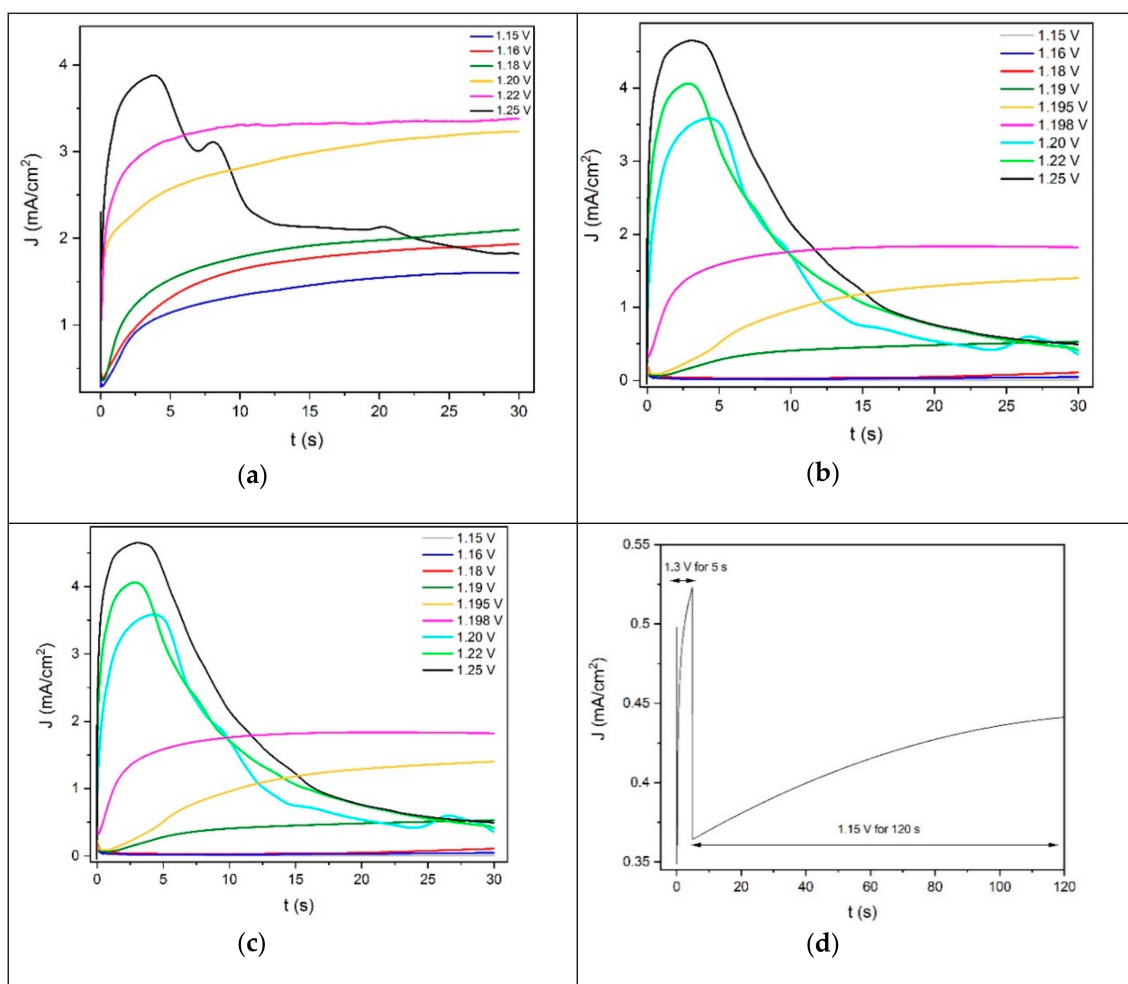
Figure 2. Chronoamperograms of EDOT solution at various potentials for 30 s on (**a**) gold, (**b**) palladium and (**c**,**d**) ITO.

Figure 2 shows the current density–time plots for the potentiostastic electropolymerization of PEDOT on Au, Pt and ITO. On gold, the depositions performed between 1.15 V and 1.22 V (Figure 2a) were characterized by a similar trend, which could be divided into

two different regions. The general features of these curves were similar to those reported in the literature [40–45].

Initially, in the first region, the current density variation followed a $t^{-1/2}$ law. This behavior is related to the diffusion-limited oxidation of the monomer. This process consists of the diffusion of EDOT from the solution towards the electrode. Then, the molecules of the monomer oxidize and return to the solution, where the oligomerization process occurs in front of the surface of the electrode. The formation of an oligomeric high-density region leads to the deposition of cluster deposits onto the substrate, creating the growing nuclei [28]. These processes occurred during the time at which the current density was minimal (induction time).

After the induction time, in the second region, the current density increased and reaches a plateau. This behavior of the chronoamperogram is generally attributed to the process of nucleation and growth [40].

The lowest current density plateau was recorded at 1.15 V. The current density plateau value increased by increasing the deposition potential. This may indicate the deposition of a higher amount of PEDOT on the gold electrode by increasing the oxidative deposition potential value. The current density–time curve obtained by depositing PEDOT at 1.25 V for 30 s followed a trend that only partially overlapped with those previously described. Indeed, after 5 s of deposition, the current density reached a maximum peak. Then, the current density decreased, bringing about a noisy signal that did not set to a plateau value. This may suggest that the deposition of PEDOT diverts on gold from the nucleation and growth model previously described, starting from a deposition potential of 1.25 V. A homogeneous film of PEDOT was obtained on gold after 30 s of deposition in the potential range of 1.15–1.25 V.

The deposition performed between 1.15 V and 1.198 V on palladium (Figure 2b) showed the same regions previously described in the case of the gold substrate. This suggests that the nucleation and growth process of PEDOT on palladium in the potential range of 1.15–1.198 V followed a behavior similar to the one taking place on gold from 1.15 V to 1.22 V. At higher potentials (1.20–1.25 V, Figure 2b), the chronoamperometric behavior changed also in the case of the palladium electrode, and the current density reached a peak instead of a plateau. Therefore, the deposition of PEDOT on palladium in the potential range of 1.198–1.25 V seemed to follow the exact same trend of the one taking place on gold-on-silicon from 1.25 V. A homogeneous film of PEDOT was obtained on palladium in potentiostatic conditions after 30 s of deposition, starting from 1.19 V. On the contrary, a high-quality coating of the polymer on gold was deposited at lower potentials, starting from 1.15 V. Therefore, it can be said that the deposition of PEDOT in potentiostatic route is favored on gold.

Figure 2c shows the current density–time curves related to the deposition of PEDOT on ITO for 30 s at different potentials. Once again, the same trend was observed, and the two main regions were individuated as in the case of Au and Pd. This suggests that the potentiostatic nucleation and growth process of PEDOT on ITO between 1.2 V and 1.25 V follows the same behavior described on gold from 1.15 V to 1.22 V and on palladium between 1.15 V and 1.198 V. On the contrary, the PEDOT deposition on ITO at 1.3 V differed from this trend. Indeed, after reaching a minimum value, the increase in the current density as a function of time was nearly negligible since the curve remained substantially flat. This is evidence of the fact that the nucleation process of PEDOT on ITO at 1.3 V is much more favored than the growth of the nuclei. The potentiostatic deposition of PEDOT on ITO in the range between 1.2 V and 1.3 V for 30 s produced non-homogeneous dark blue spots on the surface of the electrode. A homogeneous and high-coverage film was obtained by applying the onset oxidative potential value (1.3 V) for 5 s, in order to enhance the nucleation process. Then, the potential was switched at a lower value (1.15 V) for 120 s, enabling the growth of the nuclei (Figure 2d).

2.3. Raman, Visible, SEM, ESEM and AFM Characterization

An investigation of the microstructure of the electropolymerized PEDOT films was performed by SEM, ESEM and AFM analysis. Microscopy acquisitions were captured for each of the different samples, meaning the polymer deposited on diverse substrates: Pd, Au and ITO. The obtained micrographs are displayed in Figure 3, Figures S1 and S2.
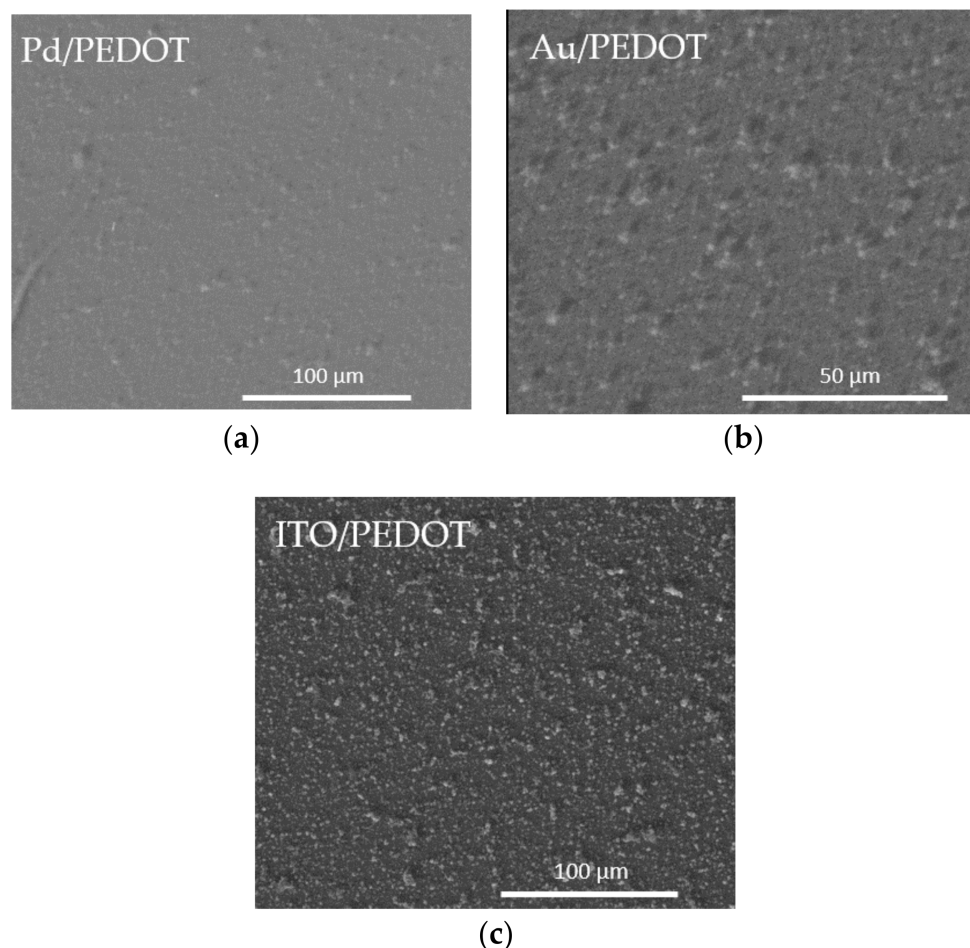
Figure 3. ESEM images of the PEDOT films on (**a**) Pd, (**b**) Au, (**c**) ITO.

The morphology appeared rough and dense, with highly visible cluster sites and uniform particle sizes (Figure 3, Figures S1 and S2). The difference between the two metallic substrates (Figure 3a,b) was negligible. On the contrary, the PEDOT films on ITO evidenced a more indented pattern, suggesting a greater contribution from nucleation. This effect can be related to the ITO surface's higher roughness, with respect to the metal ones. The Raman spectra confirmed the presence of PEDOT in all the samples. As seen from Figure 4a, the bands at 440 cm^{-1}, 992 cm^{-1} and the broadband at 1240–1270 cm^{-1} were assigned to the C–O–C deformation, oxyethylene ring deformation and Cα–Cα inter-ring stretching, respectively. In particular, the peculiar band at 1427 cm^{-1} due to symmetric Cα=Cβ (–O) stretching indicated a high level of conjugation in the structure of PEDOT [46–48]. The visible spectrum of the PEDOT coating on ITO (Figure 4b) showed the characteristic broadband dip in the absorption signal at approximately 400–700 nm, which may be related to the π–π^* transitions of thiophene ring [48].

(**a**) (**b**)
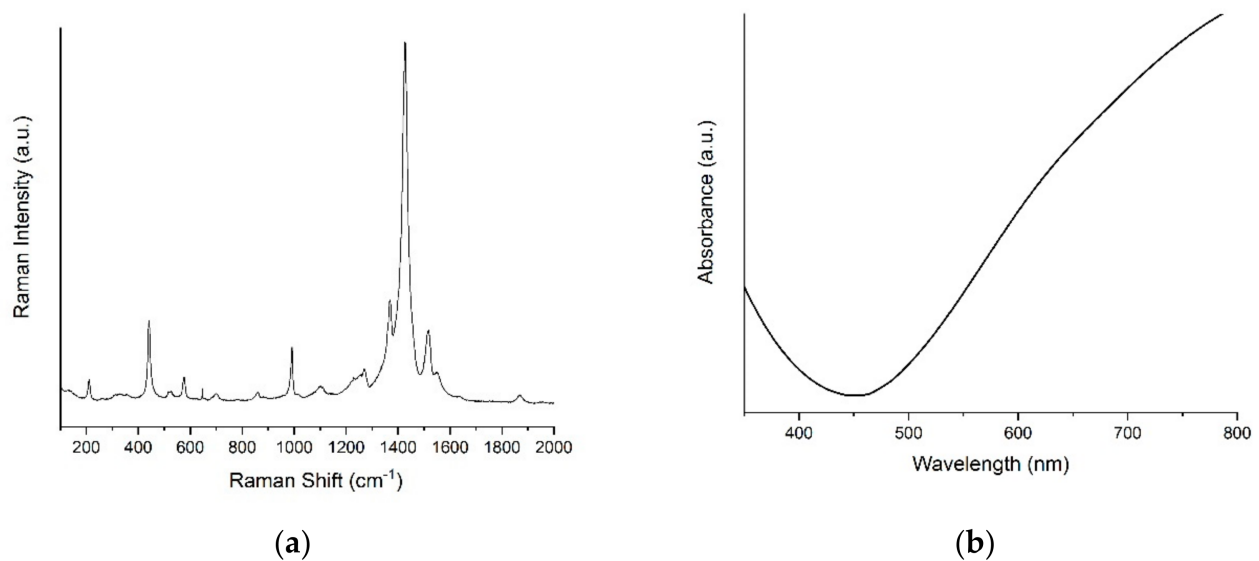
Figure 4. (**a**) Raman spectra of PEDOT/Pd, (**b**) visible spectrum of PEDOT/ITO.

2.4. Copper Electrodeposition

The previously electropolymerized PEDOT samples underwent copper metallization, described by Equation (1).

$$Cu_{aq}^{2+} + SO_4^{2-}{}_{aq} + 2e^- \rightleftharpoons Cu_s + SO_4^{2-}{}_{aq} \tag{1}$$

The Cu^{2+} ions were reduced by an electrochemical one-step process on the polymer coated substrates in an acidic electrolyte solution (1.5 M H$_2$SO$_4$ and 0.5 M CuSO$_4$, pH ranging between 1 and 1.5). Potentiostatic and galvanostatic methods were both investigated, exploring different parameters combinations, in order to obtain a uniform layer of copper with a thickness between 1 and 4 μm [49,50]. In particular, the copper depositions on PEDOT/Pd, PEDOT/Au and PEDOT/ITO were performed at −0.8 V for 300 s, −0.007 A for 600 s and −0.9 V for 600 s, respectively. Figure 5 shows the copper deposition curves on the different samples. An example of a produced sample, including the schematic representation of the layers, is reported in Figure 6.
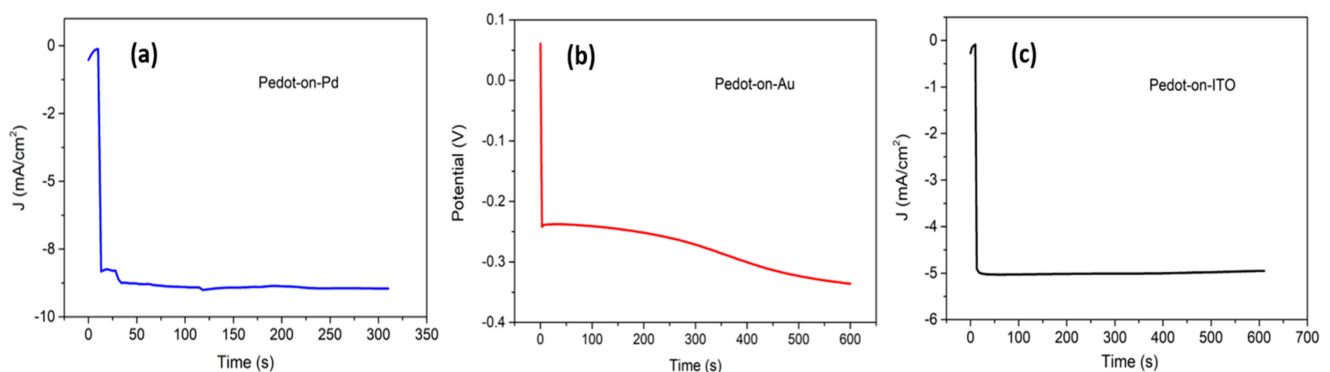
Figure 5. Curves of the copper deposition on three different working electrodes: (**a**) PEDOT/Pd, (**b**) PEDOT/Au, (**c**) PE-DOT/ITO. The electrodepositions were accomplished in a one-compartment, three-electrode electrochemical cell, with Pt wire as the counter electrode and an Ag wire as the reference electrode.
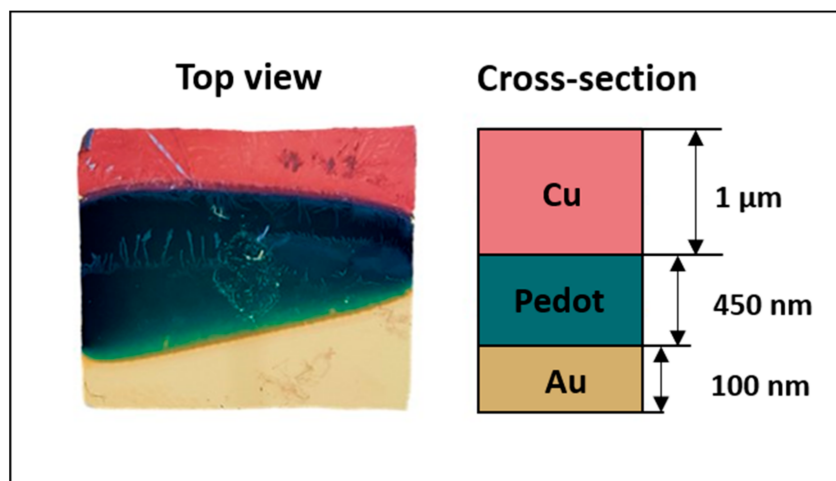
Figure 6. Image of the specimen Cu/PEDOT/Au.

2.5. Electrical Impedance Spectroscopy

Electric impedance spectroscopy was used to characterize the PEDOT–Cu hybrid systems obtained (Figure 7 and Figure S3). Two-electrode measurements were performed on all the samples, by contacting one electrode to the conductive substrate (Pd, Au, ITO) and the other to the copper layer on PEDOT. Contacts were obtained connecting copper thin wires to the sample with a small amount of silver paste. The sandwich-like systems presented an ohmic behavior all over the wide range of frequencies analyzed. The PEDOT–Cu device developed on the palladium and gold substrates was characterized by a resistance of 240 Ω cm^2 and 335 Ω cm^2, respectively. On the contrary, the hybrid system obtained on ITO showed a higher resistance (8×10^3 Ω cm^2), possibly due to the lower conductivity of the substrate.
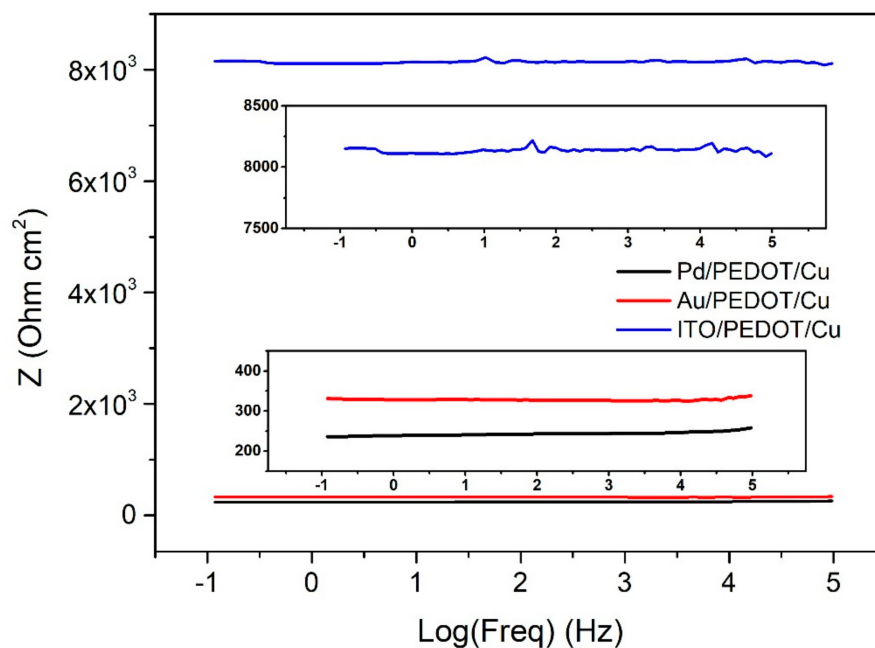
Figure 7. Bode plot of the PEDOT/Cu device, obtained on the three different substrates (Pd in black, Au in red, ITO in blue). Areas of interest are magnified in the two insets, which help in visualizing the Z values.

3. Conclusions

In the present study, we evaluated the optimal electrochemical conditions to obtain a hybrid Cu/PEDOT electronic solid-state device. The deposition of PEDOT was studied on different substrates (ITO, thin films of gold and palladium on silicon wafers) by both potentiostatic and potentiodynamic techniques. The first one produced high-quality deposits on the metal substrates but did not seem to be the optimum process to obtain PEDOT films on ITO. Smooth and homogeneous coatings of the conductive polymer on Au/Si and Pd/Si were also obtained with the potentiostatic route, starting from 1.15 V and 1.19 V in the case of gold and palladium, respectively. Chronoamperometric experiments confirmed a change in the nucleation and growth process over 1.198 V and 1.22 V for Au and Pd, respectively. The potentiostatic deposition of PEDOT on ITO produced non-homogeneous dark blue spots on the surface of the electrode. Instead, a high-coverage polymeric film was obtained on ITO by firstly applying an oxidative potential pulse (1.3 V for 5 s), then growing the polymer at 1.15 V for 120 s.

Therefore, the optimal electrochemical conditions were set to obtain homogeneous PEDOT films on all the substrates. Raman, visible, ESEM, SEM and AFM characterization confirmed the high quality of the conductive polymeric coatings. Then, a further layer of copper was electrodeposited on PEDOT films on the different electrodes. In this way, a hybrid electronic solid-state device was obtained by means of electrochemical methods only. Electrical impedance spectroscopy analysis confirmed the high conductivity of the PEDOT–Cu device and its ohmic behavior over a wide range of frequencies analyzed. This further expands the possible applications of electrochemically deposit PEDOT, especially to obtain systems prone to be used as electrodes in stacked devices.

Supplementary Materials: The following are available online at https://www.mdpi.com/article/10.3390/surfaces4020015/s1, Figure S1: SEM images of (**a**) the PEDOT film on Au and (**b**) the cross section of the polymeric deposit on Au, Figure S2: (**a**) AFM analysis of PEDOT film on Au (the horizontal lines 1-2 are to be intended as references for the plot profile (Figure S2b). (**b**) Plot profile of PEDOT film on Au observed from the two different horizontal lines present in Figure S2a. (**c**) 3D view of the AFM analysis, Figure S3: (**a**) Curves of the Copper deposition on three different working electrodes: Pd, Au and ITO. (**b**) Electrical Impedance Spectroscopy of the Substrate/Cu devices, (Pd in black, Au in red, ITO in blue).

Author Contributions: Conceptualization, C.F.; investigation, M.V., G.P., A.S. and R.G.; writing—original draft preparation, M.V. and W.G.; writing—review and editing, M.V., A.S., W.G. and C.F.; supervision, W.G. and C.F.; project administration, M.I.; funding acquisition, M.I. All authors have read and agreed to the published version of the manuscript.

Funding: This research was funded by the PRIN ("Progetti di Ricerca di Rilevante Interesse Nazionale"), which made possible the project "Novel Multilayered and Micro-Machined Electrode Nano-Architectures for Electrocatalytic Applications (Fuel Cells and Electrolyzers)", grant number 2017YH9MRK. The authors also acknowledge Regione Toscana POR CreO FESR 2014–2020—Azione 1.1.5 sub-azione a1—Bando 1 "Progetti Strategici di ricerca e sviluppo", which made possible the projects "Innovativi processi di produzione a basso impatto ambientale di catene in acciaio e alluminio" (ACAL 4.0), CUP 3553.04032020.158000165_1385, CIPE D14E20006260009 and "Arte, Moda e arredo in un Processo Elettrochimico innovativo con controllo da Remoto 4.0—Circular Ecofriendly" (A.M.P.E.R.E.), CUP 3553.04032020.158000223_1538, CUP CIPE D14E20006370009.

Institutional Review Board Statement: Not applicable.

Informed Consent Statement: Not applicable.

Data Availability Statement: The data presented in this study are available on request from the corresponding author.

Conflicts of Interest: The authors declare no conflict of interest.

References

1. Poverenov, E.; Li, M.; Bitler, A.; Bendikov, M. Major effect of electropolymerization solvent on morphology and electrochromic properties of PEDOT films. *Chem. Mater.* **2010**, *22*, 4019–4025. [CrossRef]
2. Seshadri, V.; Wu, L.; Sotzing, G.A. Conjugated Polymers via Electrochemical Polymerization of Thieno[3,4-b]thiophene (T34bT) and 3,4-Ethylenedioxythiophene (EDOT). *Langmuir* **2003**, *19*, 9479–9485. [CrossRef]
3. Ohsawa, M.; Hashimoto, N.; Takeda, N.; Tsuneyasu, S.; Satoh, T. Bending reliability of transparent electrode of printed invisible silver-grid/PEDOT:PSS on flexible epoxy film substrate for powder electroluminescent device. *Microelectron. Reliab.* **2020**, *109*, 113673. [CrossRef]
4. Ohsawa, M.; Hashimoto, N.; Takeda, N.; Tsuneyasu, S.; Satoh, T. Flexible powder electroluminescent device on transparent electrode of printed invisible silver-grid laminated with conductive polymer. *Flex. Print. Electron.* **2020**, *5*. [CrossRef]
5. Tadesse, M.G.; Dumitrescu, D.; Loghin, C.; Chen, Y.; Wang, L.; Nierstrasz, V. 3D Printing of NinjaFlex Filament onto PEDOT:PSS-Coated Textile Fabrics for Electroluminescence Applications. *J. Electron. Mater.* **2018**, *47*, 2082–2092. [CrossRef]
6. Gozzi, G. A study of the electroluminescence mechanism in a light-emitting composite produced with PEDOT:PSS, PVA and Zn$_2$SiO$_4$:Mn. *Opt. Mater.* **2018**, *84*, 843–851. [CrossRef]
7. Zhao, P.; Tang, Q.; Zhao, X.; Tong, Y.; Liu, Y. Highly stable and flexible transparent conductive polymer electrode patterns for large-scale organic transistors. *J. Colloid Interface Sci.* **2018**, *520*, 58–63. [CrossRef]
8. Innocenti, M.; Loglio, F.; Pigani, L.; Seeber, R.; Terzi, F.; Udisti, R. In situ atomic force microscopy in the study of electrogeneration of polybithiophene on Pt electrode. *Electrochim. Acta* **2015**, *50*, 1497–1503. [CrossRef]
9. Maeda, K.; Nitani, M.; Uno, M. Thermocompression bonding of conductive polymers for electrical connections in organic electronics. *Polym. J.* **2020**, *52*, 405–412. [CrossRef]
10. Nitani, M.; Nakayama, K.; Maeda, K.; Omori, M.; Uno, M. Organic temperature sensors based on conductive polymers patterned by a selective-wetting method. *Org. Electron.* **2019**, *71*, 164–168. [CrossRef]
11. Rivnay, J.; Inal, S.; Salleo, A.; Owens, R.M.; Berggren, M.; Malliaras, G.G. Organic electrochemical transistors. *Nat. Rev. Mater.* **2018**, *3*. [CrossRef]
12. Friend, R.H.; Gymer, R.W.; Holmes, A.B.; Burroughes, J.H.; Marks, R.N.; Taliani, C.; Bradley, D.D.C.; Dos Santos, D.A.; Bredas, J.L.; Logdlund, M.; et al. Electroluminescence in conjugated polymers. *Nature* **1999**, *397*, 121–128. [CrossRef]
13. Angner, M.; Agarwal, S.; Baudler, A.; Schröder, U.; Greiner, A. Large Multipurpose Exceptionally Conductive Polymer Sponges Obtained by Efficient Wet-Chemical Metallization. *Adv. Funct. Mater.* **2015**, *25*, 6182–6188. [CrossRef]
14. Park, J.; Kim, G.; Lee, B.; Lee, S.; Won, P.; Yoon, H.; Cho, H.; Ko, S.H.; Hong, Y. Highly Customizable Transparent Silver Nanowire Patterning via Inkjet-Printed Conductive Polymer Templates Formed on Various Surfaces. *Adv. Mater. Technol.* **2020**, *5*, 1–8. [CrossRef]
15. Wang, T.; Zhang, Y.; Liu, Q.; Cheng, W.; Wang, X.; Pan, L.; Xu, B.; Xu, H. A Self-Healable, Highly Stretchable, and Solution Processable Conductive Polymer Composite for Ultrasensitive Strain and Pressure Sensing. *Adv. Funct. Mater.* **2018**, *28*, 1–12. [CrossRef]
16. Shen, W.; Zhao, G.; Zhang, X.; Bu, F.; Yun, J.; Tang, J. Using dual microresonant cavity and plasmonic effects to enhance the photovoltaic efficiency of flexible polymer solar cells. *Nanomaterials* **2020**, *10*. [CrossRef]
17. Zhang, F.; Johansson, M.; Andersson, M.R.; Hummelen, J.C.; Inganäs, O. Polymer photovoltaic cells with conducting polymer anodes. *Adv. Mater.* **2002**, *14*, 662–665. [CrossRef]
18. Xia, Y.; Zhang, H.; Ouyang, J. Highly conductive PEDOT:PSS films prepared through a treatment with zwitterions and their application in polymer photovoltaic cells. *J. Mater. Chem.* **2010**, *20*, 9740–9747. [CrossRef]
19. Shi, H.; Liu, C.; Jiang, Q.; Xu, J. Effective Approaches to Improve the Electrical Conductivity of PEDOT:PSS: A Review. *Adv. Electron. Mater.* **2015**, *1*, 1–16. [CrossRef]
20. Wei, T.C.; Chen, S.H.; Chen, C.Y. Highly conductive PEDOT:PSS film made with ethylene-glycol addition and heated-stir treatment for enhanced photovoltaic performances. *Mater. Chem. Front.* **2020**, *4*, 3302–3309. [CrossRef]
21. Li, J.; Qin, J.; Liu, X.; Ren, M.; Tong, J.; Zheng, N.; Chen, W.; Xia, Y. Enhanced organic photovoltaic performance through promoting crystallinity of photoactive layer and conductivity of hole-transporting layer by V2O5 doped PEDOT:PSS hole-transporting layers. *Sol. Energy* **2020**, *211*, 1102–1109. [CrossRef]
22. Morvillo, P.; Parenti, F.; Diana, R.; Fontanesi, C.; Mucci, A.; Tassinari, F.; Schenetti, L. A Novel Copolymer from Benzodithiophene and Alkylsulfanyl-Bithiophene: Synthesis, Characterization and Application in Polymer Solar Cells. *Solar Energy Mater. Solar Cells* **2012**, *104*, 45–52. [CrossRef]
23. Marcaccio, M.; Paolucci, F.; Fontanesi, C.; Fioravanti, G.; Zanarini, S. Electrochemistry and Spectroelectrochemistry of Polypyridine Ligands: A Theoretical Approach. *Inorg. Chim. Acta* **2007**, *360*, 1154–1162. [CrossRef]
24. Lupu, S.; Javier, F.; Xavier, F. Sinusoidal voltage electrodeposition and characterization of conducting polymers on gold microelectrode arrays. *J. Electroanal. Chem.* **2012**, *687*, 71–78. [CrossRef]
25. Kumar, D.; Sharma, R.C. Advances in conductive polymers. *Eur. Polym. J.* **1998**, *34*, 1053–1060. [CrossRef]
26. Sapp, S.A.; Sotzing, G.A.; Reynolds, J.R. High Contrast Ratio and Fast-Switching Dual Polymer Electrochromic Devices. *Chem. Mater.* **1998**, *10*, 2101–2108. [CrossRef]
27. Fontanesi, C.; Baraldi, P.; Marcaccio, M. On the Dissociation Dynamics of the Benzyl Chloride Radical Anion. An Ab Initio Dynamic Reaction Coordinate Analysis Study. *J. Mol. Struct. THEOCHEM* **2001**, *548*, 13–20. [CrossRef]

28. Tamburri, E.; Orlanducci, S.; Toschi, F.; Terranova, M.L.; Passeri, D. Growth mechanisms, morphology, and electroactivity of PEDOT layers produced by electrochemical routes in aqueous medium. *Synth. Met.* **2009**, *159*, 406–414. [CrossRef]

29. Groenendaal, L.; Jonas, F.; Freitag, D.; Pielartzik, H.; Reynolds, J.R. Poly(3,4-ethylenedioxythiophene) and its derivatives: Past, present, and future. *Adv. Mater.* **2000**, *12*, 481–494. [CrossRef]

30. Shirakawa, H.; Louis, E.J.; MacDiarmid, A.G.; Chiang, C.K.; Heeger, A.J. Synthesis of electrically conducting organic polymers: Halogen derivatives of polyacetylene, (CH)x. *J. Chem. Soc. Chem. Commun.* **1977**, 578–580. [CrossRef]

31. Higgins, T.M.; Coleman, J.N. Avoiding Resistance Limitations in High-Performance Transparent Supercapacitor Electrodes Based on Large-Area, High-Conductivity PEDOT:PSS Films. *ACS Appl. Mater. Interfaces* **2015**, *7*, 16495–16506. [CrossRef] [PubMed]

32. Dietrich, M.; Heinze, J.; Heywang, G.; Jonas, F. Electrochemical and spectroscopic characterization of polyalkylenedioxythiophenes. *J. Electroanal. Chem.* **1994**, *369*, 87–92. [CrossRef]

33. Mishra, S.; Kumar, A.; Venkatesan, M.; Pigani, L.; Pasquali, L.; Fontanesi, C. Exchange Interactions Drive Supramolecular Chiral Induction in Polyaniline. *Small Met.* **2020**, *4*, 1–10. [CrossRef]

34. Fullerene-bisadducts, C.C.; Nishimura, T.; Tsuchiya, K.; Ohsawa, S.; Maeda, K.; Yashima, E.; Nakamura, Y.; Nishimura, J. Macromolecular Helicity Induction on a Poly (Phenylacetylene). *J. Am. Chem. Soc.* **2004**, *126*, 11711–11717. [CrossRef]

35. Mitzi, D.B.; Chondroudis, K.; Kagan, C.R. Organic-inorganic electronics. *IBM J. Res. Dev.* **2001**, *45*, 29–45. [CrossRef]

36. Sakmeche, N.; Aeiyach, S.; Aaron, J.J.; Jouini, M.; Lacroix, J.C.; Lacaze, P.C. Improvement of the electrosynthesis and physicochemical properties of poly(3,4-ethylenedioxythiophene) using a sodium dodecyl sulfate micellar aqueous medium. *Langmuir* **1999**, *15*, 2566–2574. [CrossRef]

37. Downard, A.J.; Pletcher, D. A study of the conditions for the electrodeposition of polythiophen in acetonitrile. *J. Electroanal. Chem.* **1986**, *206*, 147–152. [CrossRef]

38. Heinze, J.; Rasche, A.; Pagels, M.; Geschke, B. On the origin of the so-called nucleation loop during electropolymerization of conducting polymers. *J. Phys. Chem. B* **2007**, *111*, 989–997. [CrossRef]

39. Chang, B.Y. Analysis of the singular point of cyclic voltammograms recorded with various scan rates. *J. Electrochem. Sci. Technol.* **2017**, *8*, 244–249. [CrossRef]

40. Randriamahazaka, H.; Noe, V.; Chevrot, C. Erratum to "Nucleation and growth of poly (3,4-ethylenedioxythiophene) in acetonitrile on platinum under potentiostatic conditions". *J. Electroanal. Chem.* **1999**, *476*, 34257071. [CrossRef]

41. Randriamahazaka, H.; Noël, V.; Chevrot, C. Nucleation and growth of poly(3,4-ethylenedioxythiophene) in acetonitrile on platinum under potentiostatic conditions. *J. Electroanal. Chem.* **1999**, *472*, 103–111. [CrossRef]

42. Chao, F.; Costa, M.; Tian, C. Modification of poly(3-methylthiophene) (PMeT) structure during electrochemical doping-undoping, studied by in situ atomic force microscopy (ECAFM). *Synth. Met.* **1995**, *75*, 85–94. [CrossRef]

43. Lukkari, J.; Alanko, M.; Heikkilä, L.; Laiho, R.; Kankare, J. Nucleation and Growth of Poly(3-methylthiophene) on Indium-Tin Oxide Glass by Scanning Tunneling Microscopy. *Chem. Mater.* **1993**, *5*, 289–296. [CrossRef]

44. Schrebler, R.; Grez, P.; Cury, P.; Veas, C.; Merino, M.; Gómez, H.; Córdova, R.; Del Valle, M.A. Nucleation and growth mechanisms of poly (thiophene) Part 1. Effect of electrolyte and monomer concentration in dichloromethane. *J. Electroanal. Chem.* **1997**, *430*, 77–90. [CrossRef]

45. Hillman, A.R.; Mallen, E.F. Nucleation and growtn of polythiophene films on gold electrodes. *J. Electroanal. Chem.* **1987**, *220*, 351–367. [CrossRef]

46. Wu, D.; Zhang, J.; Dong, W.; Chen, H.; Huang, X.; Sun, B.; Chen, L. Temperature dependent conductivity of vapor-phase polymerized PEDOT films. *Synth. Met.* **2013**, *176*, 86–91. [CrossRef]

47. Ely, F.; Matsumoto, A.; Zoetebier, B.; Peressinotto, V.S.; Hirata, M.K.; Sousa, D.A.; Maciel, R. Handheld and automated ultrasonic spray deposition of conductive PEDOT: PSS films and their application in AC EL devices. *Org. Electron.* **2014**, *15*, 1062–1070. [CrossRef]

48. Nie, T.; Zhang, K.; Xu, J.; Lu, L.; Bai, L. A facile one-pot strategy for the electrochemical synthesis of poly(3,4-ethylene dioxythiophene)/Zirconia nanocomposite as an effective sensing platform for vitamins B2, B6 and C. *J. Electroanal. Chem.* **2014**, *717*, 1–9. [CrossRef]

49. Giurlani, W.; Berretti, E.; Lavacchi, A.; Innocenti, M. Thickness determination of metal multilayers by ED-XRF multivariate analysis using Monte Carlo simulated standards. *Anal. Chim. Acta* **2020**, *1130*, 72–79. [CrossRef]

50. Giurlani, W.; Berretti, E.; Innocenti, M.; Lavacchi, A. Measuring the Thickness of Metal Coatings: A Review of the Methods. *Coatings* **2020**, *10*, 1211. [CrossRef]